13.4

The cascade matrix electron flow amplifier based on an electron multiplier concentrator

© E.A. Il'ichev[1], A.E. Kuleshov[1], P.V. Minakov[2], G.N. Petrukhin[1], G.S. Rychkov[1], A.N. Demidova[1], D.A. Korlyakov[1]

[1] National Research University of Electronic Technology (MIET), Zelenograd, Russia
[2] Skobeltsyn Institute of Nuclear Physics, Moscow State University, Moscow, Russia
E-mail: mstlena2@mail.ru

Received December 7, 2022
Revised December 7, 2022
Accepted February 3, 2023

The design and operation of a cascade matrix electron flow amplifier based on an electron concentrator multiplier is considered. Unlike classical microchannel plates, the proposed amplifier can provide a high density of output current, which also allows it to be used as a field cathode in vacuum microelectronics of giga and terahertz ranges.

Keywords: Microchannel plate, secondary emission, screening, electron concentrator multiplier, field cathode.

DOI: 10.21883/TPL.2023.04.55875.19454

Electron flow amplifiers are of paramount importance in instrumentation engineering (especially in the field of development of high-sensitivity amplifiers of weak electron flows). A microchannel plate still remains the most widely used solution in this field [1,2]. However, owing to the presence of high-resistance channels and to the saturation effect associated with them, a microchannel plate operates in the range of very weak currents (no higher than a microampere) [3]. Matrix electron flow amplifiers providing an amplified current density of $10-100\,\mathrm{A/cm^2}$ are needed in certain applications. The use of such amplifiers as field emitters in the development of high-speed vacuum microelectronic circuits is especially promising [4]. Matrix amplifiers operating based on secondary electron emission from a diamond film are a good fit in this context. An electron multiplier concentrator (EMC) [5] is an elementary cell of an amplifier of the mentioned kind. An EMC is a through tapering hole in a conducting plate with its walls being coated with *p*-type polycrystalline diamond. The primary electron flow penetrating into this hole from the wide end reaches its walls and produces secondary electrons in diamond. Since the work function of diamond is low, a fraction of these electrons leaves the film and exit the hole via its narrow end under the influence of an electric field. Figure 1, *a* presents the photographic images of a matrix electron flow amplifier (MEFA, left) and its EMC cell formed in a silicon plate with a thickness of $470\,\mu\mathrm{m}$ (right). The gain factor of a MEFA is $30-50$. However, in order to amplify a weak initial current to a density of $100\,\mathrm{A/cm^2}$ or more, one needs to raise the gain to 10^3-10^6, which can be done only by constructing a MEFA cascade with accurate matching of EMC outputs of the first MEFA and inputs of a similar EMC of the next MEFA (Fig 1, *b*, left panel). The presented design has a drawback in that secondary electrons emitted from a diamond film, which have an energy below 1 eV at the moment of emission, return back to the same diamond film after entering into a strong field of the preceding MEFA. This drawback may be rectified by covering EMC inputs with a graphene film, which transmits electrons with energies above 100 eV freely [6]. Unfortunately, a graphene film starts absorbing electrons at an energy below 100 eV; this translates into a required uniformity of graphene films in all EMC cells. Ideally, graphene should be single-layer, but a reliable procedure for fabrication of such films with an area greater than $1\,\mathrm{mm^2}$ has not been proposed yet. The use of films with a nonuniform thickness translates into a certain spread of gain factors between EMC cells, and this is unacceptable for the electron flow that carries two-dimensional data.

In the present study, we consider a screening method that is free from the mentioned drawbacks. It consists in separating a MEFA from the previous one by a mirror MEFA of the same type (MEFA* in Fig. 1, *b*, right panel). A MEFA* differs from a common MEFA not only in its mirror positioning, but also in the lack of a diamond film and the presence of a dielectric surface coating, which is colored green in Fig. 1, *b* (a color version of the figure is provided in the online version of the paper), on the EMC output side. We call the proposed design a flow amplifier and denote it as UP, assuming that an UP cell is a pair formed by EMCs of a primary MEFA and a mirror MEFA*.

Let us demonstrate that a cascade connection of UP cells makes it possible to achieve the needed gain. In order to do this, we examine the trajectories of electrons moving from an UP1 cell to the next UP2 cell (Fig. 2; the indicated sizes are in millimeters) with the use of SIMION-8. The studied cascade amplifier fragment is axially symmetric with respect to line OO'. Cells UP1 and UP2 are also regarded as electrodes 2 and 3, which are bordered on the left and on the right by electrodes 1 and 4 that are needed to verify the screening efficiency. U_i is the voltage at electrode i

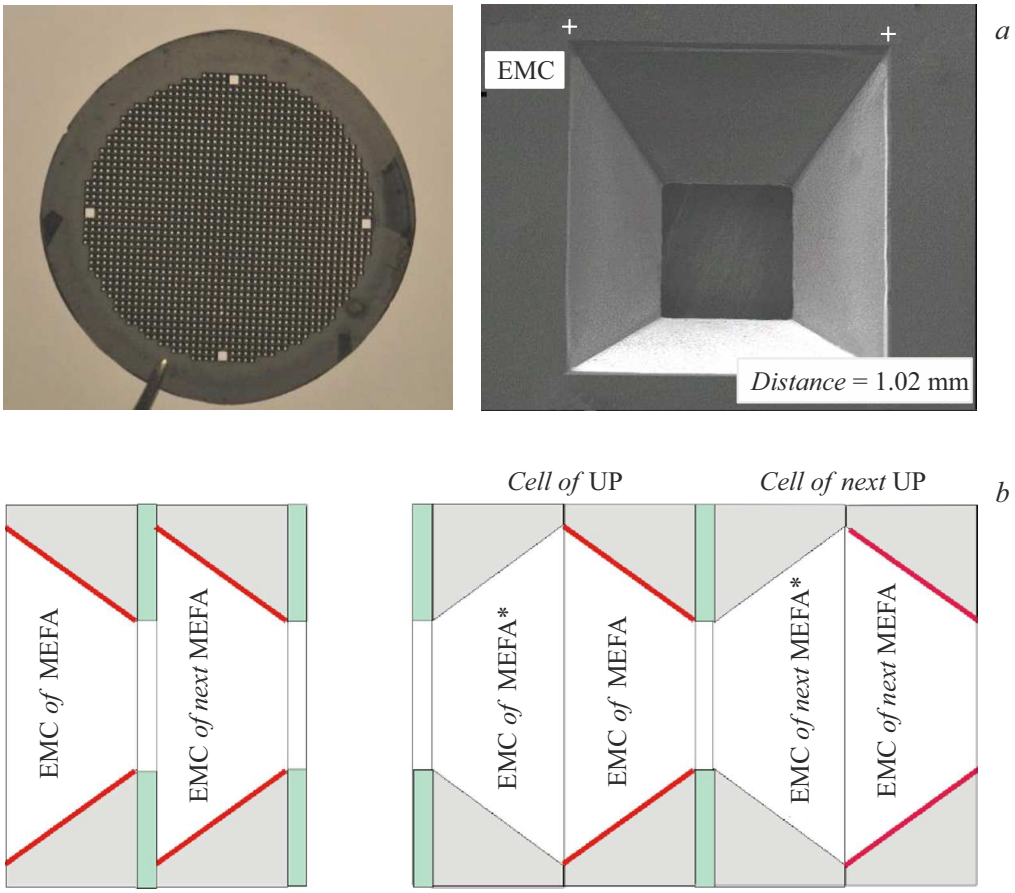

Figure 1. *a* — Matrix electron flow amplifier MEFA (left) and its cell, electron multiplier concentrator EMC (right); *b* — simple design of a cascade amplifier (left) and design of a cascade amplifier with neutralization of the influence of the electric field of the preceding MEFA (right).

($i = 1-4$). The electron trajectories and equipotential lines of the electric field were determined at voltages

$$U_1 = 0.3U_2, \quad 2U_2 = U_3, \quad U_4 = 1.3U_3 \qquad (1)$$

and $U_2 = 500$ V. Owing to its smallness, the initial energy of secondary electrons at the surface of a diamond film of cell UP1 was assumed to be 0 eV [7]. Numbers written in cursive are the values of electric potential (in keV) of equipotential lines denoted by dots. It follows from the analysis of trajectories that electrons leaving the cavity of cell UP1 acquire an energy approximately equal to qU_3 — qU_2 (here and elsewhere, q is the electron charge). This is the energy with which they affect the diamond film of cell UP2, producing secondary electrons in it. In geometric terms, the surfaces of cells UP1 and UP2 coated with a diamond film may be regarded as identical point sets G_1 and G_2, and the trajectories may be viewed as mapping f of set G_1 into G_2. With G_1 being identical to G_2, we have $fG_1 \subset G_1$. It follows from the set theory (e.g., the Cantor theorem [8]) that sequential application of mapping f should yield in this case an invariant set that transforms into itself. This implies that secondary electrons are produced in a chain of UP amplifiers and affect a diamond film (in the next UP) within the bounds of one and the same region.

The geometry of trajectories of electrons and equipotential lines of the electric field remains unchanged if condition (1) is satisfied to within an additive constant. It is important for the nature of mapping $fG_1 \subset G_1$ to be largely unaffected by voltages U_1 and U_4 under conditions $U_1 < U_2$ and $U_3 < U_4$, which are established in a cascade UP connection. Dependence $h_2 = g(h_1, U_1, U_4)$, where h_1 and h_2 are the distances from the start and end trajectory points to the bases of truncated cones coated with a diamond film (Fig. 2), was examined to estimate the degree of influence of these voltages. Quantities h_1 and h_2 do not define points in sets G_1 and G_2 unambiguously, but uniquely determine circles O_{h1} and O_{h2} located at distances h_1 and h_2, respectively, from the bases of truncated cones. This is sufficient to assess the nature of mapping f of set G_1 into G_2. Plots of function $h_2 = g(h_1, U_1, U_4)$ at fixed U_1 and U_4 are presented in Fig. 3. It can be seen that $h_2 \in [c, d]$ at all times if $h_1 \in [a, b]$; notably, $a < c$ and $b > d$. This implies that $fG_1 \subset G_1$ holds true under the chosen external voltages if G_1 and G_2 are identical; i.e., the required condition is satisfied. The insignificance of

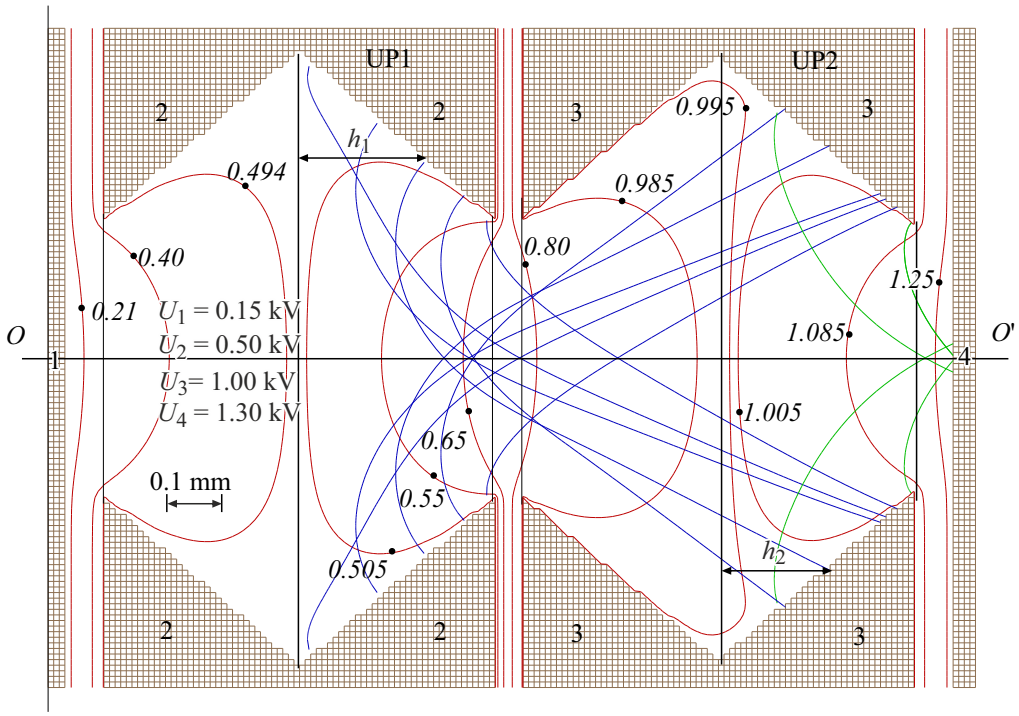

Figure 2. Positioning of electron trajectories (blue curves) and equipotential lines of the electric field (brown curves) in cells UP1, UP2 and between them. Green curves denote the trajectories of secondary electrons that leave cell UP2 under the influence of the electric field produced by electrode 4. A color version of the figure is provided in the online version of the paper.

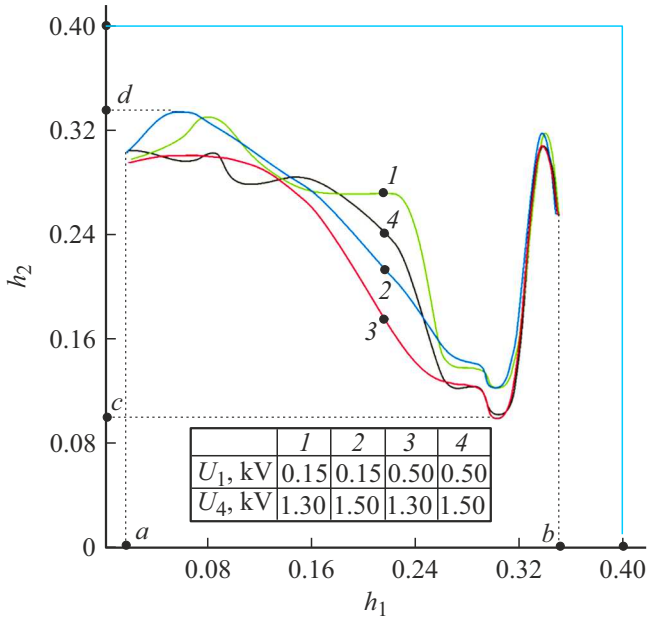

Figure 3. Plots of functions $h_2 = \mathrm{g}(h_1, U_1, U_4)$ at fixed U_1 and U_4.

the influence of U_1 and U_4 on mapping f is attributable to the fact that the nature of trajectories is defined largely by the voltages at UP1 and UP2. Specifically, trajectories are mostly confined to the region bounded by 505 V and 995 V equipotential lines at $U_2 = 500$ V and $U_3 = 1000$ V.

All calculations were performed under the assumption that UP cells are axially symmetric. However, the overall nature of behavior of electrons is also retained if an EMC has the shape of a truncated pyramid.

With U_i $(i = 1{-}4)$ being varied and condition (1) satisfied to within an additive constant, trajectories retain their shape; the only changing parameter is electron energy $E_q = (U_3{-}U_2)q$, which affects secondary emission coefficient $K_q(E_q)$. If a cascade amplifier contains n cascades UP_i $(i = 1{-}n)$, its gain is $K_M = \Pi_{i=2}^{n} K_i$, where K_i is the gain in cascade i. Voltage U_f applied to an amplifier and its optimum distribution between cascades, which is needed to maximize K_M, is an important parameter. Using the Lagrangian method, we find that the distribution should be uniform (i.e., the voltage difference between cascades should be $U_f/(n-1)$; consequently, $K_i = K_q\big(qU_f/(n-1)\big)$ $(i = 2{-}n)$). However, number n may not be the optimum one for a fixed U_f . The determination of optimum $n_{\max}$ comes down to finding the maximum of function $K_M(n) = \Big(K_q\big(qU_f/(n-1)\big)\Big)^{n-1}$ in n. The dependence of K_q on E_q was determined in [7]. It may be presented, as a first approximation, as $K_q = gE_q$, where $g = 0.02{-}0.05\,\mathrm{eV}^{-1}$ (the electron energy is measured in eV). It is easy to find that $n_{\max} = [gqU_f/e] + 1$ and $K_{\max} = \exp(n_{\max} - 1)$. Here, e is the Napier's constant $(e = 2.7\ldots)$ and square brackets denote the integral part

of a number in these brackets. At $U_f = 1\,\text{kV}$, $n_{\max} = 8-19$ and $K_{\max} \approx 10^3-6\cdot 10^7$. With limit $n < n_{\max}$ introduced, one should choose the greatest n on the basis that $K_M(n)$ increases monotonically for these n.

Thus, a cascade matrix amplifier is produced simply by connecting tightly adjoining amplifiers UP_i $(i = 1-n)$ into a cascade. Voltages U_i may be supplied in various ways (e.g., via side strip contacts formed in a single fabrication cycle with a MEFA itself).

The development of UP amplifiers with cells of a minimum size, which depends on the microelectronic processing level, is of interest. Let us consider the case when an EMC in the form of a truncated pyramid is formed in a silicon plate with thickness d. If the ratio of bases of a truncated pyramid is 1:4, side length W of the input EMC base is $W = 4d\,\text{ctg}\,54.7^\circ \approx 2.8d$. Leading foreign manufacturers work with plates with a thickness of $50-100\,\mu$m [9]. Certain manufacturers (e.g., Wafer World) produce plates with a thickness of $10-30\,\mu$m and a diameter no less than 25.4 mm [10]. At a thickness of $10\,\mu$m, we obtain $W \approx 28\,\mu$m, which yields a cell density of $\sim 10^5\,\text{cm}^{-2}$. Naturally, the diamond coating should be nanocrystalline in this case. Cells may also be made more compact through the use of polycrystalline and single-crystalline p-type diamond membranes. These provide both a maximum output current density and a high density of cells (in excess of $10^7\,\text{cm}^{-2}$).

As was already noted, the use of graphene films is a sound solution to the screening problem, but these films need to be uniform. No well-proven techniques for fabrication of films with an area in excess of $1\,\text{mm}^2$ are available at present, although graphene single crystals with an area of $\sim 10\,\text{mm}^2$ were produced in a laboratory environment [11]. In fact, an entire matrix of 12 000 graphene single crystals, which was transferred onto a silicon plate, was produced experimentally [12]. Overall, this offers prospects of development of a more compact and more efficient cascade matrix electron flow amplifier.

Funding

This study was supported financially by the Russian Foundation for Basic Research as part of research project No. 20-38-90125.

Conflict of interest

The authors declare that they have no conflict of interest.

References

[1] T. Cremer, B.W. Adams, M. Aviles, C. Lyashe, J. Minot, M.A. Popecki, T. Rivera, M.E. Stochaj, A.U. Mane, J.W. Elam, M. Gebhard, O.H. Siegmund, Proc. SPIE, **11118**, 111180M (2019). DOI: 10.1117/12.2530037

[2] L. Giudicotti, M. Bassan, R. Pasqualotto, A. Sardella, Rev. Sci. Instrum., **65** (1), 247 (1994). DOI: 10.1063/1.1144791

[3] A.B. Berkin, V.V. Vasil'ev, Tech. Phys., **53** (2), 272 (2008). DOI: 10.1134/S1063784208020217.

[4] E.A. Il'ichev, A.E. Kuleshov, G.N. Petrukhin, P.V. Minakov, G.S. Rychkov, V.V. Sen', E.G. Teverovskaya, Tech. Phys. Lett., **47**, 503 (2021). DOI: 10.1134/S1063785021050230.

[5] E.A. Il'ichev, A.E. Kuleshov, E.A. Poltoratsky, G.S. Rychkov, Diamond Rel. Mater., **20** (1), 23 (2010). DOI: 10.1016/j.diamond.2010.11.002

[6] E. Il'ichev, V. Khaustov, A. Kuleshov, D. Migunov, P. Minakov, R. Nabiev, G. Petrukhin, E. Teverovskaya, G. Rychkov, Diamond Rel. Mater., **94**, 209 (2019). DOI: 10.1016/j.diamond.2019.03.005

[7] V.V. Dvorkin, N.N. Dzbanovsky, N.V. Suetin, E.A. Poltoratsky, G.S. Rychkov, E.A. Il'ichev, S.A. Gavrilov, Diamond Rel. Mater., **12** (12), 2208 (2003). DOI: 10.1016/S0925-9635(03)00320-0

[8] P.S. Aleksandrov, *Vvedenie v teoriyu mnozhestv i obshchuyu topologiyu* (Nauka, M., 1977), p. 183 (in Russian).

[9] D. Bodnar', Kompon. Tekhnol., No. 11, 116 (2012) (in Russian).

[10] J.-E. Hong, Y. Lee, S.-I. Mo, H.-S. Jeong, J.-H. An, H.-E. Song, J. Oh, J. Bang, J-H. Oh, K.-H. Kim, Adv. Mater., **33** (41), 2103708 (2021). DOI: 10.1002/adma.202103708

[11] S.B. Salk, R.R. Pandey, P.H.Q. Pham, D. Zhou, W. Wei, G. Cochez, D. Vignaud, E. Pallecchi, P.J. Burke, H. Happy, Nanomaterials, **11** (10), 2528 (2021). DOI: 10.3390/nano11102528

[12] M.A. Giambra, V. Mišeikis, S. Pezzini, S. Marconi, A. Montanaro, F. Fabbri, V. Sorianello, A.C. Ferrari, C. Coletti, M. Romagnoli, ACS Nano, **15** (2), 3171 (2021). DOI: 10.1021/acsnano.0c09758